

COMPARATIVE SYNTHESIS, CHARACTERIZATION OF Cu-DOPED ZnO NANOPARTICLES AND THEIR ANTIOXIDANT, ANTIBACTERIAL, ANTIFUNGAL AND PHOTOCATALYTIC DYE DEGRADATION ACTIVITIES

S. A. KHAN^{a*}, F. NOREEN^b, S. KANWAL^c, G. HUSSAIN^d

^aDepartment of Chemistry, University of Management & Technology, Lahore-54770, Pakistan

^bDepartment of Botany, GC University for Women Faisalabad-38000, Pakistan

^cDepartment of Biochemistry, University of Agriculture Faisalabad-38000, Pakistan

^dInstitute of Chemistry, University of Punjab Lahore-54000, Pakistan

In this study, synthesis, characterization, antioxidant, antibacterial, antifungal and photocatalytic properties of copper-doped zinc oxide nanoparticles have been investigated. Undoped ZnO and Copper doped ZnO nanoparticles have been synthesized by using co-precipitation method 1 (M1 Naps) and method 2 (M2 Naps). The synthesized un-doped ZnO, M1 Naps, and M2 Naps were characterized by X-ray diffraction (XRD), energy-dispersive X-ray spectroscopy (EDX), scanning electron microscope (SEM) and Ultraviolet-visible (UV-Vis) spectroscopic techniques. The antibacterial and antifungal activity of M1 Naps and M2 Naps was determined by the agar diffusion method while their antioxidant properties were assessed through DPPH radical scavenging, ferric reducing antioxidant power (FRAP), ferric thiocyanate (FTC) and total phenolic content (TPC) assays. Photocatalytic disintegration activity of M1 Naps and M2 Naps was determined by the degradation of Acid Black 234 (AB) dye. Results of XRD, EDX and SEM confirmed the successful synthesis, crystalline nature, spheroid to the rod-like shape of un-doped ZnO, M1 Naps, and M2 Naps. The average grain size of un-doped ZnO, M1 Naps, and M2 Naps was 16.72 nm, 17.49 nm, and 20.73 nm respectively. Photocatalytic studies revealed that both nanoparticles are a good catalyst for effective degradation of Acid Black 234. M1 Naps and M2 Naps nanoparticles were exhibited remarkable antioxidant activity. Significant antibacterial and antifungal activity was shown by M2 Naps against bacterial strains (*E. coli*, *S. aureus*, *Klebsiella* and *B. subtilis*) and fungal strains (*A. niger* and *T. harzianum*) with ZOI of (13±0.09, 14±0.01, 18±0.07 and 20±0.10) and (17±0.07 and 24±0.08) respectively in contrast to standard drug. Hence, Synthesized Cu-doped ZnO nanoparticles demonstrated splendid photocatalytic, antibacterial, antifungal and antioxidant potential, indicating that they are good candidates for future therapeutic applications.

(Received June 21, 2017; Accepted August 25, 2017)

Keywords: Synthesis; characterization; antioxidant; antibacterial; antifungal; photocatalytic

1. Introduction

From recent years, ZnO nanoparticles are getting much more attention due to their diverse applications [1]. Now days, prototype ZnO nanoparticles are using as delivering systems for vaccines and anti-cancer drugs [2]. ZnO nanoparticles are being used as antimicrobial agents, as an additive in industrial products and as a photo-catalyst to disintegrate the organic materials [3]. But ZnO nanostructures are being widely investigated till now to enhance their potential applications

* Corresponding author: shakilahmad56@gmail.com

in the field of biomedicine [2]. As the functionality and efficiency of ZnO nanoparticles and nanostructures can be improved by increasing and modifying their surface area by adding some dopants materials i.e. biomolecules and transition metals (Mn, Fe, Cr, Cu) at nanoscale [4]. Through surface modification with biomolecules and transition metals, the ZnO nanoparticles could be used as biosensors, antimicrobial, antioxidants, drug delivery systems and bio-imaging materials [1,4,5]. Different methods have been developed for the fabrication of ZnO and transition metal doped ZnO nanoparticles [6]. The doping of semiconductor metals divided into two types, (i) Cationic doping, (ii) Anionic doping, the doping of a cation to metal oxide is known as cationic doping e.g. Cu, Na, Mg, Co, Al, Ni, Mn, V, Cr etc. [5-9]. Whereas the doping of an anion to metal oxide is known as anionic doping e.g. S, C and N. Among all the dopants, doping of ZnO Naps with Cu greatly alter the optical, morphological structural, magnetic, electrical, and biological properties of the ZnO Naps [10,11]. ZnO nanoparticles doped with Cu have shown remarkable improvement in different properties i.e. electrical conductivity [12], magnetic [13], biological [14], gas sensing [15], optical properties and mechanical strength [16]. ZnO nanoparticles exhibit photocatalytic activity but when ZnO doped with Cu, then it shows enhanced photocatalytic activities because its surface area is enhanced [17]. The aims of present research were involved to synthesize and characterize the Cu-doped ZnO nanoparticles. Furthermore, their evaluations of antibacterial, antifungal, antioxidant and photocatalytic dye degradation activities were also involved to be determined.

2. Materials and methods

The current research work was performed at the Research and Development Laboratory of Shafi Reso Chemicals Lahore and biochemistry laboratory, University of Management and technology, Lahore, Pakistan. All chemicals and reagents used were procured from Sigma-Aldrich and Merck and were of analytical grade. These reagents included butylated hydroxytoluene, BHT (99.07777%); 2, 2-diphenyl-1-picrylhydrazyl radical DPPH (90.0%); Folin-Ciocalteu reagent (2N), linoleic acid and catechin.

Energy dispersive x-ray technique was employed for the determination of the composition and morphology of the synthesized un-doped ZnO and Cu-doped ZnO nanoparticles from method 1 and method 2. In addition, characterization of the crystalline structure of the nanoparticles was done using the XRD i.e. PANalytical X'Pert diffractometer instrument with Cu-K α radiation (wavelength 0.154 nm) operating at 40 kV and 30 mA. Measurements were scanned for diffraction angles (2θ) ranging from 20° to 90° with a step size of 0.02° and a time per step of 1 s. The absorption spectrum and band gap energies of the synthesized nanoparticles were analyzed by UV-visible spectrophotometer (Spectra Flash SF 550, Data color Inc., USA). Their morphological features were determined using SEM (Jeol, 5910LV).

2.1 Synthesis of un-doped ZnO Nanoparticles

Un-doped or pure zinc oxide (ZnO) nanoparticles were synthesized by a co-precipitation method using zinc nitrate hexahydrate ($\text{Zn}(\text{NO}_3)_2 \cdot 6\text{H}_2\text{O}$), sodium carbonate (Na_2CO_3) and sodium hydroxide (NaOH) as starting materials. 14.427 g of zinc nitrate was dissolved in 50 ml distilled water to prepare 1M zinc nitrate solution. This solution was placed on a magnetic stirrer for 1 hr at room temperature (25°C). A basic solution was prepared separately by dissolving 4 g of NaOH and 10.6 g of Na_2CO_3 in 50 ml distilled water in order to maintain the pH value of the solution at 14. The basic solution was then added drop by drop to the initial solution under constant stirring and the reaction was allowed to proceed for 2h at room temperature (25°C) to obtain white gel like precipitates. At the end of the reaction, the solution was placed intact and allowed to settle for overnight at 25°C . The white precipitates were settled down at the bottom and the floating solution was discarded carefully. The white precipitates were washed with distilled water several times until they became neutral. After washing, the final precipitates were placed in an oven for drying at 120°C for 2h. After drying, the precipitates were ground in an agate mortar. Finally, the collected nanoparticles were heated in a furnace at 500°C for 2 hr [9].

2.2 Synthesis of Cu-doped ZnO nanoparticles according to method 1 (M1 Naps)

The same procedure is adopted for copper doping except for the addition of 1M Cu (NO₃)₂ to Zn (NO₃)₂.6H₂O solution. Zinc nitrate, 14.427 g was dissolved in 50 ml distilled water to prepare 1M zinc nitrate solution. Then the solution was placed on magnetic stirrer under constant stirring at room temperature (25 °C) for 1 hr. A 1M solution of copper nitrate was prepared by dissolving 0.3624 g of copper nitrate in 50 ml distilled water and then placed it under constant stirring at room temperature (25 °C) using a magnetic stirrer for 2 hr. The solutions of zinc nitrate and copper nitrate were mixed after complete dissolution. A basic solution was prepared separately by dissolving 4 g of sodium hydroxide and 10.6 g of sodium carbonate in 50 ml distilled water to maintain the pH value of the solution to 14. This basic solution was then added drop by drop to the combined solution of zinc nitrate and copper nitrate under constant stirring and this reaction were allowed to proceed for 2h at room temperature to obtain white gel like precipitates. At the end of the reaction, the solution was placed and allowed to settle for overnight. The white precipitates were settled down at the bottom and the floating solution on it was then thrown out carefully. The white precipitates were washed with distilled water several times until they became neutral. After washing, the final precipitates were placed in an oven for drying at 120 °C for 2 hr. These dried precipitates were then ground in an agate mortar. Finally, the collected nanoparticles were heated in a furnace at 500 °C for 2 hr [9].

2.3 Synthesis of Cu-doped ZnO nanoparticles according to method 2 (M2 Naps)

The copper doped ZnO nanoparticles were also prepared by using Zinc nitrate hexahydrate (Zn(NO₃)₂.6H₂O), copper nitrate trihydrate (Cu (NO₃)₂.3H₂O) and sodium hydroxide (NaOH) as starting materials. 1M solution Zinc nitrate solution was prepared by dissolving 14.427 g of zinc nitrate in 50ml distilled water. After that, the solution was placed under constant stirring at room temperature (25 °C) using magnetic stirrer for 1h. Then, a 1M solution of copper nitrate was prepared by dissolving 0.3624 g of copper nitrate in 50 ml distilled water and then placed it also under constant stirring at room temperature (25 °C) using a magnetic stirrer for 2 hr. Both the solutions of zinc nitrate and copper nitrate were mixed after stirring. Then, a 1M solution of sodium hydroxide was added dropwise to the combined solution of zinc nitrate and copper nitrate to adjust the pH value 14 of the solution. When the pH value reached to 14, this solution was allowed to settle for overnight. White, gelatinous precipitates were settled down at the bottom. Filtration of these precipitates was done and washed with distilled water several times until they became neutral. Then these precipitates were dried in an oven at 120 °C for 2 hr. After drying, these precipitates were ground in an agate mortar. Finally, these nanoparticles were heated in a furnace at 200 °C for 3 hr [9].

2.4 Antioxidant Potential Evaluation

2.4.1 DPPH free Radical Scavenging Assay

The known antioxidant value of BHT was compared with unknown values of synthesized M1 and M2 Naps of 2, 2-diphenyl-1-picrylhydrazyl according to the method of Khan *et al.*, [18].

2.4.2 Ferric thiocyanate (FTC) assay

The inhibitory effect of the synthesized M1 and M2 Naps on linoleic acid peroxidation was studied by using the thiocyanate method of Ijaz *et al.*, [19].

2.4.3 Ferric reducing antioxidant power (FRAP) assay

Antioxidant potential of M1 and M2 nanoparticles was assessed by evaluating the ferric reducing antioxidant power assays as described by Ijaz *et al.*, [19].

2.4.4 Total phenolic content (TPC) assay

The total phenolic content of the M1 and M2 Naps nanoparticles was determined by the colorimetric method as described by Khan *et al.*, [20].

2.5 Antibacterial potential evaluation

The antibacterial potential of the synthesized Cu-doped ZnO nanoparticles was examined by Agar well diffusion method as described by [21,22]. The bacterial strains used for antibacterial potential were *Staphylococcus aureus* (ATCC 25923), *Bacillus subtilis* (ATCC 9637), *Klebsiella* (ATCC 10031) and *Escherichia coli* (ATCC 25922). These bacterial strains were obtained from PCSIR laboratories complex, Lahore, Pakistan. A standard antibiotic drug used for positive control was Cephadrine.

2.6 Antifungal potential evaluation

Antifungal potential of synthesized Cu-doped ZnO nanoparticles was explored by using the method as described by [23,24]. The fungal strains that were used for the determination of antifungal potential in this research work were *Aspergillus niger* (ATCC 16404), *Aspergillus flavus* (ATCC 9643), and *Trichoderma harzianum* (ATCC 20846). These fungal strains were already cultured in the microbiology lab of Industrial Biotechnology Division of NIBGE Faisalabad, Pakistan. Standard drug “Terbinafine hydrochloride” was used as a positive control.

2.7 Photocatalytic degradation activity

Photocatalytic degradation activity of the Cu-doped ZnO nanoparticles was estimated by the disintegration of Acid Black 234 (AB1) dye under sunlight irradiation. For this assay, 0.005 g of synthesized CuO nanoparticles was dispersed in 5 mL distilled water in a test tube and then ultrasonicated. Ten milliliters of 13 mM Acid Black 234 dye solution was added to 5 mL of the Copper doped ZnO nanoparticles solution and kept in the dark for 30 min. To obtain adsorption-desorption stage, Cu-doped ZnO nanoparticles suspension with Acid Black 234 was exposed at different time intervals (20, 40, 60, 80 min). This experiment was performed between 11 am to 1 pm. The suspensions obtained were centrifuged for two min, and the concentration of Acid Black 234 in the resultant solution was monitored in the wavelength range of 200-800 nm in a UV-visible spectrophotometer. Distilled water was used as a reference.

2.8 Statistical analysis

Statistical analysis was done by one-way or two-way ANOVA and the Tukey post-test using Graph Pad Prism v6.04 software (GraphPad Software, Inc., La Jolla, CA, USA). Differences were considered statistically significant at $p < 0.05$. Group sizes are indicated in the figure legends. All values are expressed as mean \pm SD.

3. Results

3.1 X-RAY diffraction analysis

X-ray diffraction is a nondestructive analytical technique that gives detailed information about the chemical composition and crystallographic structure of natural and synthesized materials [12]. Figure 1 shows the XRD pattern of undoped ZnO nanoparticles. The sharp diffraction peaks in the XRD pattern distinctly shows the crystalline nature of the sample [25]. Standard diffraction peaks represent the crystal structure of ZnO is hexagonal wurtzite structure according to the standard JCPDS data card (JCPDS Card No: 00-001-1136). There are no diffraction peaks of other impurities detected which proves that the substance only belongs to the ZnO. The average grain size of the un-doped ZnO nanoparticles was calculated from the three most intense peaks using Debye-Scherrer's formula. The resultant average grain size of un-doped ZnO nanoparticles was 16.72 nm.

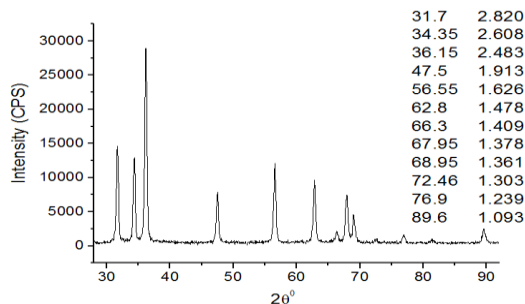


Fig. 1. XRD spectrum of un-doped ZnO nanoparticles

The typical XRD patterns of synthesized Cu-doped ZnO nanoparticles with method 1 (M1 Naps) were shown in Figure 2. The intense peaks show the hexagonal wurtzite structure of ZnO according to the JCPDS Card No: 00-001-1136. The hexagonal wurtzite structure of ZnO is the most stable phase of ZnO. As seen in this XRD pattern below, there are additional peaks correlates to Cu-related phases and impurities. These peaks are due to the incorporation of Cu into the Zn interstitial spaces [25]. The average grain size of the synthesized Cu-doped ZnO nanoparticles by method 1 is 17.49 nm that was calculated from the three most intense peaks using Debye-Scherrer's formula.

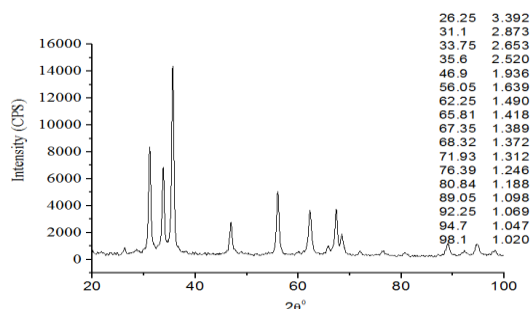


Fig. 2. XRD spectrum of Cu-doped ZnO from method 1 (M1 Naps)

Fig. 3 shows the XRD pattern for the Cu-doped ZnO synthesized by method 2 (M2 Naps). The hexagonal wurtzite structure of the ZnO was confirmed from the intense peaks pattern of XRD spectrum. XRD spectrum of M2 Naps also shows the same pattern of peaks as were observed for M1 Naps XRD spectrum but there are extra sharp peaks corresponding to Cu due to its more doping in ZnO. The existence of these peaks implies that Cu ions were incorporated into the Zn interstitial sites. The average grain size of the sample synthesized by method 2 is 20.73 nm that was calculated from the three most intense peaks using Debye-Scherrer's formula.

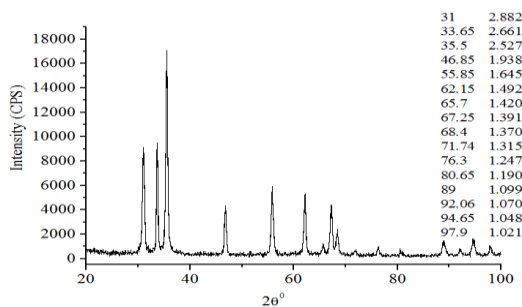


Fig. 3. XRD spectrum of Cu-doped ZnO synthesized from method 2 (M2 Naps)

3.2 Scanning electron microscope (SEM) studies

The surface morphology of the un-doped ZnO, Cu-doped ZnO nanoparticles synthesized by method 1 (M1 Naps) and method 2 (M2 Naps) was studied by SEM and their graph is shown in Figure 4 (a and b), (c) and (d) respectively. It clearly shows that the average size of the nanoparticles is in the range of nanometer size. Figure 4 (a) & (b) illustrates that the synthesized undoped ZnO nanoparticles are homogeneous in nature and equally distributed over the surface. While Figure 4 (c) and (d) show that the shape of the doped particles is changed from the spheroid to rod-like. The average size of the particles observed by SEM is below 100 nm which is found in accordance with the XRD results. The SEM results show that size and shape of the ZnO nanoparticles depend on the Cu additive. These findings are found in close agreement with previous reports [16].

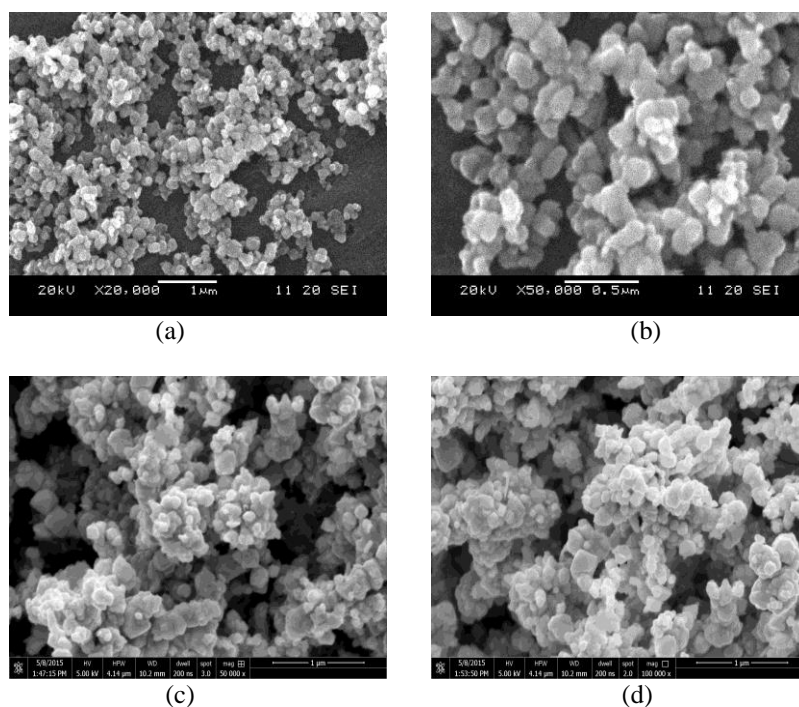


Fig. 4: (a and b) SEM micrographs of pure ZnO nanoparticles, (c) Cu-doped ZnO nanoparticles from method 1, (d) Cu-doped ZnO nanoparticles from method 2

3.3 Energy-dispersive X-ray analysis (EDX)

EDX was carried out to analyze the chemical composition and formation of un-doped ZnO, Cu-doped ZnO nanoparticles from method 1 (M1 Naps) and method 2 (M2 Naps). The typical EDX spectra of undoped ZnO nanoparticles, M1 Naps, and M2 Naps were shown in Figure 5 (a), (b) and (c) respectively. EDX spectra clearly confirmed the formation of un-doped ZnO, M1 Naps, and M2 Naps. Beside this, EDX spectra confirmed the presence of chemical constituents (Zn-55.10% and O-45.90%) in un-doped ZnO nanoparticles, (Cu-2.70%, Zn-46.57% and O-2.70) in M1 Naps and (Cu-5.10%, Zn-45.37% and O-49.53%) in M2 Naps. In addition to these chemical components, traces of Silicon (Si) were also observed in undoped ZnO from the substrate and M1 Naps but not present in M2 Naps as shown in Figure 5. The EDX peak positions were consistent with Zinc Oxide, and the sharp peaks of EDX indicated that the synthesized nanoparticles had a crystalline structure. The strong intensity and narrow width of ZnO diffraction peaks indicate that the resultant products were highly crystalline in nature. These findings are in close agreement with previous reports [25] but with the slight difference due to variations in chemical composition.

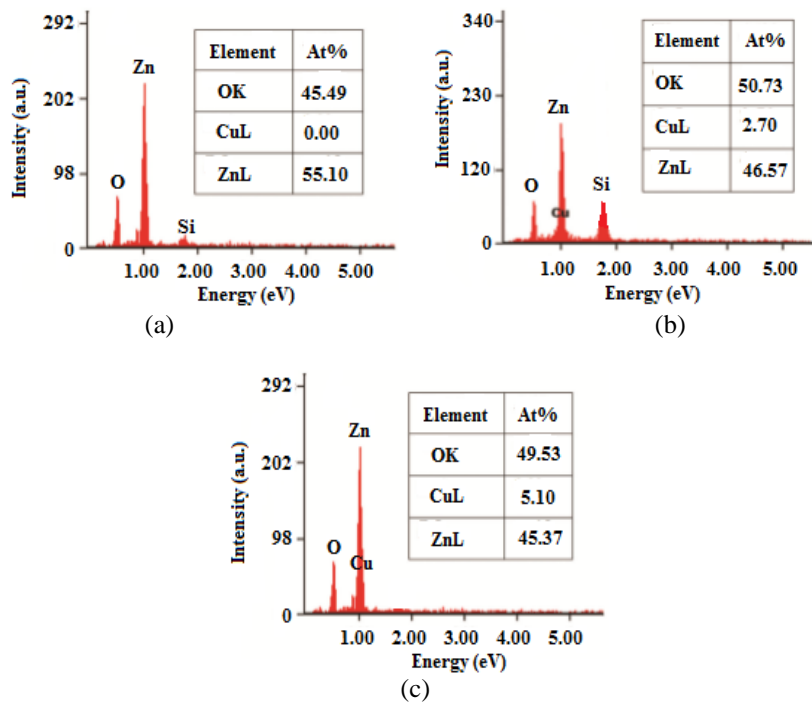


Fig. 5. EDX spectrum of undoped ZnO Naps (a), Cu-doped ZnO Naps synthesized from method 1 (b), Cu-doped ZnO Naps synthesized from method 2 (c)

3.4 Band gap energy data

The band gap of the undoped ZnO, Cu-doped ZnO nanoparticles synthesized by method 1 (M1 Naps) and 2 (M2 Naps) were obtained by plotting absorptivity $(\alpha h\nu)^2$ as a function of energy ($h\nu$) and presents in Figure 6 (a), (b) and (c) respectively. Extrapolating the linear portion of the curve to absorption gives the band gap energies which are 3.37 eV, 3.36 eV and 3.33 eV for undoped ZnO, M1 Naps and M2 Naps respectively. The decrease in band gap energies was found from un-doped ZnO to M2 Naps. The reason behind this decreasing of band gap energy from 3.37 eV to 3.30 eV is due to the doping of Cu in M1 Naps and M2 Naps. M2 Naps have less band gap energy value as compared to M1 Naps as the concentration of Cu in M2 Naps is more doped as compared to M1 Naps [4] Undoped ZnO and M1 Naps have more band gap value because of the Si impurity [25] as shown in Figure 5.

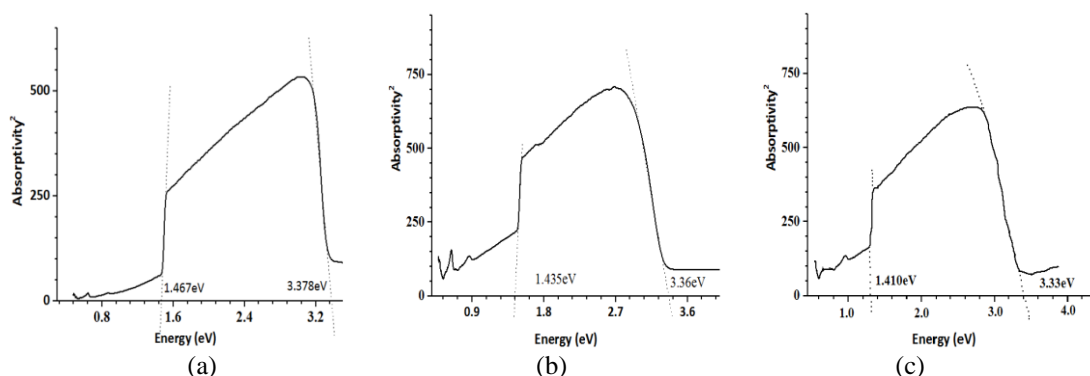


Fig. 6. Band gap energy graph of un-doped ZnO Naps (a), Cu-doped ZnO nanoparticles synthesized by Method 1(b) and 2 (c)

3.5 Photo-catalytic dye degradation

The disintegration of organic dye by the Cu-doped ZnO nanoparticles synthesized by method 1 (M1 Naps) and method 2 (M2 Naps) is shown in Figure 7 (A) and (B). M1 Naps have disintegrated the Acid Black 234 in 80 minutes. While M2 Naps were disintegrated the same quantity of Acid Black 234 in 60 minutes only. This is because of the fact that M2 Naps have a more crystalline structure in comparison to M1 Naps. As the degradation/decomposition rate of the organic dye totally depends on morphological and crystal structure of the photochemical catalyst [19]. The active sites of photocatalysts can be increased by increasing surface area and crystalline structure; these, in turn, increase the effectiveness of photocatalytic reactions by separating electron-hole pairs [19]. In the first step, M1 Naps and M2 Naps come in contact with light, creating a photo-generated electron and a hole. The photo-generated electron reacts with an oxygen molecule to form superoxide free radical in the second step. In the third step, the hole reacts with water and hydroxyl ions to produce highly mercurial hydroxyl radicals. These superoxide free radicals and hydroxyl free radicals react violently with Acid Black 234 organic dye and decompose/ decolorize it in the next step [4,19].

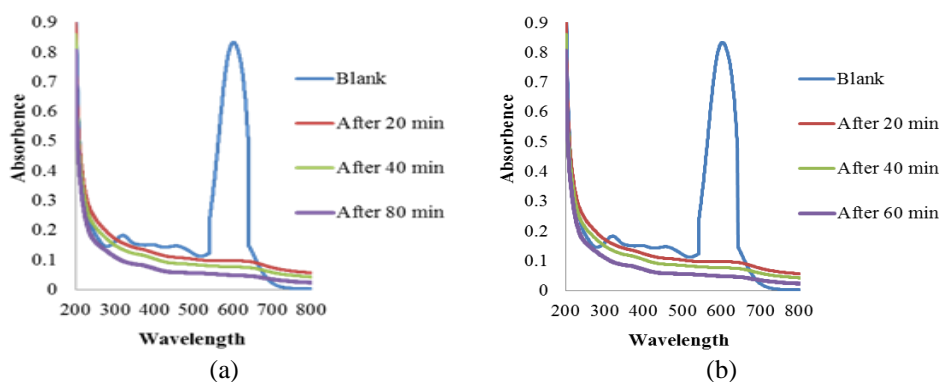


Fig. 7. Photocatalytic activity of Cu-doped ZnO nanoparticles against Acid Black 234 dye synthesized from method 1 (a) and method 2 (b)

3.6 Antioxidant activities

3.6.1 DPPH radical scavenging assay

The results of DPPH radical scavenging assay for different concentrations of Cu-doped ZnO nanoparticles are shown in Table 1 in the form of IC_{50} values. The highest IC_{50} value ($41 \pm 0.32 \mu\text{g/ml}$) was seen at a concentration of $1000 \mu\text{g/mL}$, while the lowest IC_{50} value ($85 \pm 0.23 \mu\text{g/ml}$) was obtained at a concentration of $60 \mu\text{g/mL}$ for Cu-doped ZnO nanoparticles synthesized by method 1. While in the case of Cu-doped ZnO nanoparticles synthesized by method 2, highest IC_{50} ($39 \pm 0.22 \mu\text{g/ml}$) for $1000 \mu\text{g/mL}$ and lowest IC_{50} ($78 \pm 0.25 \mu\text{g/ml}$) for $1000 \mu\text{g/mL}$ were found. Hence it is evident that the DPPH free radical scavenging increased with increasing concentration of the Cu-doped ZnO nanoparticles. At $1000 \mu\text{g/mL}$, the Cu-doped ZnO nanoparticles showed significant DPPH radical scavenging activity which was comparable to that of BHT having an IC_{50} value of $48 \pm 0.29 \mu\text{g/ml}$. This indicates that the synthesized Cu-doped ZnO nanoparticles from both methods possess high antioxidant activity in terms of scavenging DPPH free radicals.

3.6.2 Total phenolic contents (TPC)

A high percentage of total phenolic contents ($20.1 \pm 0.21 \text{ mg/100g}$ as GAE) were noticed in $1000 \mu\text{g}$ concentration while minimum total phenolic contents ($0.95 \pm 0.08 \text{ mg/100g}$ as GAE) value was observed in $60 \mu\text{g}$ of Cu-doped ZnO nanoparticles synthesized by method 1. The Same behavior was observed in different concentrations of Cu-doped ZnO nanoparticles synthesized by method 2 but greater as compared to Cu-doped ZnO nanoparticles synthesized by method 1. As a percentage of total phenolic contents varied from 1.09 ± 0.18 to $23.1 \pm 0.31 \text{ mg/100g}$ as GAE for the different concentrations ($60 \mu\text{g}$, $125 \mu\text{g}$, $250 \mu\text{g}$, $500 \mu\text{g}$ and $1000 \mu\text{g}$) of Cu-doped ZnO

nanoparticles that were synthesized from method 2. These results are shown in Table 1. The TPC activity of the Cu-doped ZnO nanoparticles increased with increasing concentration.

3.6.3 Antioxidant activity via inhibition of linoleic acid oxidation

The results of antioxidant activity of different concentrations of Cu-doped ZnO nanoparticles determined using the percentage inhibition of linoleic acid oxidation are shown in Table 1. The percentage inhibition of linoleic acid peroxidation was 18 ± 0.23 , 31 ± 0.19 , 43 ± 0.15 , 50 ± 0.17 and 63 ± 0.21 for 60 μg , 125 μg , 250 μg , 500 μg and 1000 μg of Cu-doped ZnO nanoparticles synthesized by method 1 respectively. Maximum percentage inhibition was $63\pm 0.21\%$ (for 1000 μg of CuO nanoparticles), while the minimum percentage inhibition ($18\pm 0.23\%$) was recorded for 60 μg of the nanoparticles. For Cu, doped ZnO nanoparticles synthesized by method 2, percentage inhibitions were varied from $21\pm 0.13\%$ to $65\pm 0.11\%$. More antioxidant activity via inhibition of linoleic acid oxidation was observed by Cu-doped ZnO nanoparticles that were synthesized from method 2 as compared to method 1. This is due to the fact of more doping of Cu on ZnO nanoparticles in method 2 as compared to method 1 as seen in figure 5 (c). Linoleic oxidation was significantly inhibited by the Cu-doped ZnO nanoparticles at all the levels tested, and the percentage inhibition was comparable to that of BHT which produced $61\pm 0.19\%$ inhibition.

3.6.4 FRAP assay

In the FRAP assay, the maximum antioxidant activity of (8.99 ± 0.21 $\mu\text{M}/\text{mL}$ as TE) was produced by 1000 μg while the minimum antioxidant activity (0.59 ± 0.01 $\mu\text{M}/\text{mL}$ as TE) was observed with the 60 μg of Cu-doped ZnO nanoparticles from method 1. FRAP results for 1000, 500, 250, 125 and 60 μg of Cu-doped ZnO nanoparticles from method 1 were 8.99, 4.68, 3.01, 1.88, and 0.59 $\mu\text{M}/\text{mL}$ as TE respectively. Antioxidant activity of Cu-doped ZnO nanoparticles synthesized by method 2 was varied from 0.79 ± 0.11 to 10.9 ± 0.11 $\mu\text{M}/\text{mL}$ as TE. High antioxidant results in terms of FRAP was exhibited by Cu-doped ZnO nanoparticles synthesized by method 2 in contrast to method 1. These results are shown in Table 2.

Table 1: Antioxidant activity of Cu-doped ZnO nanoparticles synthesized by method 1 and 2

Sr. No.	Concentration (μg)	DPPH IC ₅₀ ($\mu\text{g}/\text{ml}$)	FRAP ($\mu\text{M}/\text{mL}$ as TE)	TPC (mg/100g as GAE)	%Inhibition of Linoleic acid oxidation
M1 Naps					
1	60	85 ± 0.23	0.59 ± 0.01	0.95 ± 0.08	18 ± 0.23
2	125	71 ± 0.30	1.88 ± 0.12	2.01 ± 0.11	31 ± 0.19
3	250	68 ± 0.29	3.01 ± 0.09	5.01 ± 0.15	43 ± 0.15
4	500	56 ± 0.33	4.68 ± 0.19	11.2 ± 0.25	50 ± 0.17
5	1000	41 ± 0.32	8.99 ± 0.21	20.1 ± 0.21	63 ± 0.21
BHT		48 ± 0.29	-	-	61 ± 0.19
M2 Naps					
1	60	78 ± 0.25	0.79 ± 0.11	1.09 ± 0.18	21 ± 0.13
2	125	65 ± 0.36	2.08 ± 0.02	4.99 ± 0.01	35 ± 0.29
3	250	58 ± 0.25	4.01 ± 0.19	8.01 ± 0.25	48 ± 0.05
4	500	49 ± 0.20	7.40 ± 0.09	15.3 ± 0.05	56 ± 0.27
5	1000	39 ± 0.22	10.9 ± 0.11	23.1 ± 0.31	65 ± 0.11
BHT		48 ± 0.29	-	-	61 ± 0.19

Values are mean \pm SD triplicate assays. M1 Naps= Cu-doped ZnO nanoparticles synthesized by method 1, M2 Naps= Cu-doped ZnO nanoparticles synthesized by method 2

3.7 Antibacterial activity

The results of antimicrobial activity of the Cu-doped ZnO nanoparticles synthesized by both methods are depicted in Table 2 and Table 3. The Cu-doped ZnO nanoparticles from method 1 (M1 Naps) at 5 mg showed effective antimicrobial activity against *Klebsiella* and *B. subtilis*,

with zones of inhibition (ZOI) of 15 ± 0.05 mm and 17 ± 0.11 mm respectively. With 3 mg of the Cu-doped ZnO nanoparticles from method 1, effective antimicrobial activity was also seen for *Klebsiella* and *B. subtilis*, with ZOI values of 13 ± 0.04 mm and 15 ± 0.07 mm, respectively. Cu-doped ZnO nanoparticles from method 1 with 5 mg exhibited strong antibacterial activity with minimum inhibitory concentration (MIC) 0.09 and 0.04 mg/ml for *Klebsiella* and *B. subtilis* respectively. While 0.13 and 0.07 mg/ml MIC with 3 mg were observed for *Klebsiella* and *B. subtilis* respectively. Compared with the standard drug Cephadrine; it was evident that 5 mg was much more effective for *klebsiella* and *B. subtilis*. ZOIs of Cephadrine for *klebsiella* and *B. subtilis* were 12 ± 0.05 mm and 14 ± 0.09 mm respectively. In comparison to standard drug and M1 Naps, the strong bactericidal potential was exhibited by Cu-doped ZnO nanoparticles from method 2 (M2 Naps) as depicted in Table 3. M2 Naps with 5 mg concentration were found strongly active to inhibit the growth of *E. coli*, *S. aureus*, *Klebsiella* and *B. subtilis* with ZOI of 13 ± 0.09 , 14 ± 0.01 , 18 ± 0.07 and 20 ± 0.10 respectively. MIC of M2 Naps with 5 mg was ranged from 0.03-0.09 mg/ml. Hence, Cu-doped ZnO nanoparticles showed very effective broad spectrum antibacterial activity. Antibacterial results for M1 Naps and M2 Naps were presented in Table 2 and 3 respectively.

Table 2. Zones of inhibition of antibacterial test of Cu-doped ZnO nanoparticles (M1 Naps) against different bacterial strains

Bacterial Strains	Inhibition zone of diameter (mm)			MIC (mm)		
	Standard (1mg)	M1 Naps (5mg)	M1 Naps (3mg)	Standard (1mg)	M1 Naps (5mg)	M1Naps (3mg)
	<i>E. coli</i>	11 ± 0.09	08 ± 0.08	07 ± 0.04	0.30	0.80
<i>S. aureus</i>	13 ± 0.05	11 ± 0.11	08 ± 0.09	0.10	0.95	1.01
<i>Klebsiella</i>	12 ± 0.05	15 ± 0.05	13 ± 0.04	0.14	0.09	0.13
<i>B. subtilis</i>	14 ± 0.09	17 ± 0.11	15 ± 0.07	0.08	0.04	0.07

Values are mean \pm SD triplicate assays. M1 Nps = Cu-doped ZnO nanoparticles from method 1, MIC= Minimum inhibition concentration, Standard= Cephadrine

Table 3: Zones of inhibition of antibacterial test of Cu-doped ZnO nanoparticles (M2 Naps) against different bacterial strains

Bacterial Strains	Inhibition zone of diameter (mm)			MIC (mm)		
	Standard (1mg)	M2 Naps (5mg)	M2 Naps (3mg)	Standard (1mg)	M2 Naps (5mg)	M2 Naps (3mg)
	<i>E. coli</i>	11 ± 0.09	13 ± 0.09	9 ± 0.05	0.30	0.09
<i>S. aureus</i>	13 ± 0.07	14 ± 0.01	11 ± 0.08	0.10	0.08	0.85
<i>Klebsiella</i>	12 ± 0.05	18 ± 0.07	14 ± 0.05	0.14	0.07	0.11
<i>B. subtilis</i>	14 ± 0.09	20 ± 0.10	17 ± 0.06	0.08	0.03	0.05

Values are mean \pm SD triplicate assays. M2 Nps = Cu-doped ZnO nanoparticles from method 2, MIC= Minimum inhibition concentration, Standard= Cephadrine

3.8 Antifungal activity

The results of antifungal activity of the Cu-doped ZnO nanoparticles synthesized by the both methods are depicted in Table 4 and 5. The Cu-doped ZnO nanoparticles (M1 Naps) at 5 mg and 3 mg concentrations showed effective antifungal activity against only *T. harzianum* with zones of inhibition (ZOI) of 24 ± 0.05 mm and 21 ± 0.04 along with MIC of 0.08 and 0.10 mg/ml respectively. Compared with the standard drug Terbinafine hydrochloride; it was evident that 5 mg concentration of M1 Naps was much more effective. ZOIs of the standard drug were 20 ± 0.05 mm for *T. harzianum* which was less than the M1 Naps (5mg) but was comparable M1 Naps (3mg). Antifungal potential to inhibit the fungal strains was observed more by M2 Naps in contrast to M1

Naps as presented in Table 5. High fungal strains inhibition activity was experimented by M2 Naps at 5 mg with ZOI of 17 ± 0.07 and 24 ± 0.08 against *A. niger* and *T. harzianum* respectively in comparison to a standard. MIC (0.09 and 0.06 mg/ml) was exhibited by M2 Naps at 5 mg while MIC (0.29 and 0.14 mg/ml) was presented by drug against *A. niger* and *T. harzianum* respectively. More doping of the concentration of Cu on ZnO nanoparticles in the method 2 is the reason to show more antifungal activity by M2 Naps. Thus, Cu-doped ZnO nanoparticles exhibited very effective broad spectrum antifungal activity.

Table 4: Zones of inhibition of antifungal test of Cu-doped ZnO nanoparticles (M1 Naps) against different fungal strains

Fungal Strains	Inhibition zone of diameter (mm)			MIC (mm)		
	Standard (1mg)	M1 Naps (5mg)	M1 Naps (3mg)	Standard (1mg)	M1 Naps (5mg)	M1 Naps (3mg)
<i>A. niger</i>	14 ± 0.09	13 ± 0.08	10 ± 0.04	0.29	0.46	0.86
<i>A. flavus</i>	19 ± 0.05	17 ± 0.11	15 ± 0.09	0.10	0.39	0.96
<i>T. harzianum</i>	20 ± 0.05	24 ± 0.05	21 ± 0.04	0.14	0.08	0.10

Values are mean \pm SD triplicate assays. M1 Nps = Cu-doped ZnO nanoparticles from method 1, MIC= Minimum inhibition concentration, Standard= Terbinafine hydrochloride

Table 5: Zones of inhibition of antifungal test of Cu-doped ZnO nanoparticles (M2 Naps) against different fungal strains

Fungal Strains	Inhibition zone of diameter (mm)			MIC (mm)		
	Standard (1mg)	M2 Naps (5mg)	M2 Naps (3mg)	Standard (1mg)	M2 Naps (5mg)	M2 Naps (3mg)
<i>A. niger</i>	14 ± 0.09	17 ± 0.07	12 ± 0.05	0.29	0.09	0.48
<i>A. flavus</i>	19 ± 0.05	15 ± 0.10	10 ± 0.08	0.10	0.66	0.07
<i>T. harzianum</i>	20 ± 0.05	24 ± 0.08	19 ± 0.09	0.14	0.06	0.22

Values are mean \pm SD triplicate assays. M2 Nps = Cu-doped ZnO nanoparticles from method 2, MIC= Minimum inhibition concentration, Standard= Terbinafine hydrochloride

4. Discussion

ZnO and Cu-doped ZnO nanoparticles have attracted a lot of research interest because of their significant and important roles as catalyst, ceramic resistor, superconducting material, gas sensor, as well as their roles in biological fields and in the energy sector [2,5]. SEM results confirmed the nano range of the un-doped ZnO and synthesized Cu-doped ZnO nanoparticles from method 1 (M1 Naps) and 2 (M2 Naps). Results also confirmed their spherical shape for un-doped ZnO nanoparticles and spheroid to Rod like for M1 Naps and M2 Naps. These findings are in agreement with those reported in previous studies [4,9]. Results from EDX were consistent with the SEM results, and it was evident from the EDX spectrum that the Cu-doped ZnO nanoparticles were synthesized successfully. The major constituents of the nanoparticles were Zn, O, Cu and negligible impurities (Si). It was also confirmed from EDX results that the M1 Naps and M2 Naps were crystalline, based on their strong, intense, narrow width and sharp peaks in the EDX spectrum. The EDX results in the present study are similar to previously published data [9,25]. Sharp peaks of the synthesized Cu-doped ZnO nanoparticles also appeared in the XRD spectrum, which confirmed their crystalline nature and supported the EDX results. The energy band gap result for the synthesized un-doped ZnO, M1 Naps, and M2 Naps were 3.378 eV, 3.36 eV and 3.30 eV respectively but in the current study band gap data was slightly higher in un-doped ZnO and M1 Naps when compared with previously reported data. This is likely due to the effect of some

amorphous and nanostructured impurity (Si) that were present in the un-doped ZnO and M1 Naps; this was responsible for the increased energy band gap [4,25]. The nature of the synthesized Cu-doped ZnO nanoparticles (M1 Naps and M2 Naps) as a photocatalyst was evident from the disintegration phenomenon in which the organic nature commercial grade Acid Black 234 dye was degraded by the nanoparticles. The Cu-doped ZnO nanoparticles: M1 Naps and M2 Naps completely disintegrated the Acid Black 234 dye into CO₂ and H₂O within 80 minutes and 60 minutes respectively. The high disintegrative capacity of the Cu-doped ZnO nanoparticles is due to their crystalline nature, because studies have shown that the higher the crystalline nature, the higher the disintegrative ability and the disintegration rate [19].

Different amounts (1000 µg, 500µg, 250 µg, 125µg, 60µg) of the synthesized Cu-doped ZnO nanoparticles (M1 Naps and M2 Naps) were investigated for antioxidant potential through total antioxidant (DPPH radical scavenging, FRAP, inhibition of linoleic acid peroxidation and total phenolic content (TPC) assays. The results revealed concentration-dependent antioxidant effects, with 1000 µg producing the most potent antioxidant effects. Similar concentration-dependent antioxidant properties have been reported previously [3]. Interestingly, the 1000 µg of Cu-doped ZnO nanoparticles (M1 Naps, M2 Naps) produced antioxidant effects similar and comparable to that of the standard antioxidant BHT with respect to percentage inhibition of linoleic acid peroxidation and DPPH assay. All results of antioxidant activities were found in accordance with each other and were relate results with each other also. These results are in close agreement with previously reported data [8].

The Cu-doped ZnO nanoparticles (M1 Naps) at 5 mg and 1 mg produced higher antimicrobial effects than the standard drug Cephadrine in the inhibition of growth of *Klebsiella*, and *Bacillus subtilis*. While Cu-doped ZnO nanoparticles (M2 Naps) exhibited the strong and greater bactericidal effect in contrast to standard drug and M1 Naps via inhibiting the growth of the *E. coli*, *S. aureus*, *Klebsiella* and *B. subtilis*. This superior antimicrobial activity was due to the fact that the copper ions released from Cu-doped ZnO nanoparticles permeated the bacterial cell membrane and destroyed the structure of the cell membrane by attaching to the negatively-charged cell wall [4]. Copper ions and Zinc ions are involved in cross-linkage of nucleic acid strands by binding them with DNA molecule of bacteria. This results in a disordered helical structure of DNA molecule which causes denaturation of proteins and some other biochemical processes in the cell, leading to complete destruction of the bacterial cell [19]. Factors which affect the sensitivity of bacteria to Cu-doped ZnO nanoparticle are the size of particles, the temperature of synthesis of the nanoparticles, structure of bacterial cell wall, and degree of contact of the nanoparticles with bacteria [25-28].

Antifungal potential to inhibit the growth of fungal strain was exhibited by Cu-doped ZnO nanoparticles (M1 Naps and M2 Naps). But this potential more effectively and greatly was explored by M2 Naps via growth inhibiting of two fungal strains i.e. *A. niger* and *T. harzianum* while M1 Naps only inhibited the growth of *T. harzianum* effectively. M1 Naps and M2 Naps were showed the antifungal activity better as compared to the standard drug was used in this research work. Current were found in close approximate to the previously reported studies [19].

5. Conclusions

Copper doped zinc oxide nanoparticles (ZnO: Cu) were successfully synthesized by using co-precipitation technique by employing two routes of synthesis. A white color Copper doped ZnO nanoparticles were obtained. The results obtained in this study illustrate that the synthesized Cu-doped ZnO nanoparticles possess potent and desirable biological activities. Hence, it is also suggested that Cu-doped ZnO nanoparticles with efficient antimicrobial, antifungal, and antioxidant activities hold enormous potential for cosmetics, nutraceuticals as well as for pharmaceuticals.

From this study, it is also concluded that Cu-doped ZnO nanoparticles have shown the prodigious ability of photocatalytic activity by disintegrating the organic dye. In near future, these nanoparticles might be used in the cleaning of water containing organic dyes as effluents.

Acknowledgments

This work was supported by the Department of Chemistry, School of Science, University of Management and Technology, Lahore, Pakistan and SRC (Pvt) LTD. Pakistan.

References

- [1] R. Chauhan, A. Kumar, R.P. Chaudhary, *Journal of Chemical and Pharmaceutical Research* **2**(4), 178(2010)
- [2] S.P. Lau, T.S. Heng, S.F. Yu, H.Y. Yang, *Applied Physics Letters* **90**, 032509-1 (2007).
- [3] D.C. Look, *Material Science and Engineering: B* **80**(1-3), 402 (2001).
- [4] K. Kalantar, K. Kabir, F. Gharibi, S. Hatami, A. Maleki, *Journal of Medicinal and Bacteriol* **2**(1-2), 20 (2013).
- [5] G. Glaspell, P. Dutta, A. Manivanna, *Journal of Cluster Science* **16**(4), 523 (2005).
- [6] A. N. Malika, A.R. Reddy, K.S. Babu, K.V. Reddy, *Ceramics International* **40**, 12171 (2014).
- [7] Z.Q. Ma, W.G. Zhao, Y. Wang, *Thin Solid Film* **515**, 8611 (2007).
- [8] V.D. Mote, J.S. Dargad, B.N. Dole, *Nanoscience and Nano Engineering* **1**(2), 116 (2013).
- [9] S. Muthukumar, M. Ashokkumar, *Optical Materials* **37**, 671 (2014).
- [10] S. Deka, P.A. Joy, *Solid State communications* **142**, 190 (2007)
- [11] R. Saleh, N.F. Djaja, *Spectrochim Acta part A: Molecular and Biomolecular Spectroscopy* **130**, 581 (2014).
- [12] O.G. Jayakumar, H.G. Salunke, R.M. Kadam, M. Mohapatra, G. Yaswant, S.K. Kulshreshtha, *Nanotechnology* **17**, 1278 (2006).
- [13] M.E. Abrishami, A. Kompany, S.M. Hosseini, N.G. Bardar, *Journal of sol-Gel Science and Technology* **62**(2), 153 (2012).
- [14] S. Kim, J.H. Jun, K. Chao, J. Yun, K.S. Suh, T.Y. Kim, *Organic Electron* **9**, 445 (2008).
- [15] Y. Lu, J. Zhong, S. Muthukumar, Y. Chen, H.M Ng, W. Jiang, E.L. Garfunkel, *Applied Physics Letters* **83**(16), 3401 (2003).
- [16] D. Meng, X. Yu, C. Liu, X. He, Y. Wang, J. Xie, *Material Letter* **86**, 112 (2012).
- [17] S. Cimitan, S. Albonetti, L. Forni, F. Peri, D. Lazzari, *Journal of Color Interface Science* **329**, 73 (2009).
- [18] S. A. Khan, N. Rasool, M. Riaz, R. Nadeem, U. Rashid, K. Rizwan, M. Zubair, I.H. Bukhari, T. Gulzar, *Asian Journal of Chemistry* **25**(13), 7457 (2013).
- [19] F. Ijaz, S. Shahid, S.A. Khan, W. Ahmad, S. Zaman, *Tropical Journal of Pharmaceutical Research* **16**(4), 743 (2017).
- [20] S.A. Khan, S. Shahid, Z.A. Khan, A. Iqbal, *International Journal of Scientific Research and Publications* **6**(3), 529 (2016).
- [21] S.A. Khan, S. Shahid, M. Jameel, A. Ahmad, *International Journal of Pharmaceutical Chemistry* **6**(4), 107 (2016).
- [22] S. A. Khan, M. Jameel, S. Kanwal, S. Shahid, *International Journal of Pharmaceutical Science and Research* **2**(3), 29 (2017).
- [23] W. Ahmad, S.A. Khan, K.S. Munawar, A. Khalid, S. Kawanl, *Tropical Journal of Pharmaceutical Research* **16**(5), 1137 (2017).
- [24] S.A. Khan, S. Shahid, W. Ahmad, S. Ullah, *International Journal of Pharmaceutical Science and Research* **2**(2), 22 (2017).
- [25] S.A. Khan, F. Noreen, S. Kanwal, A. Iqbal, G. Hussain, *Materials Science and Engineering C* **82C**, 46 (2017).
- [26] S.A. Khan, S. Shahid, M.R. Sajid, F. Noreen, S. Kanwal, *International Journal of Advanced Research* **5**(6), 925 (2017).
- [27] S.A. Khan, S. Kanwal, A. Iqbal, W. Ahmad, *International Journal of Advanced Research* **5**(4), 1350 (2017).
- [28] G. Hussain, S.A. Khan, W. Ahmad, M. Athar, R. Saleem, *International Journal of Advanced Research* **5**(4), 234 (2017).